Beam position measurements at the TTF Linac

P. Castro
Deutsches Elektronen Synchrotron DESY
Notkestraße 85, D-22603 Hamburg, Germany

November 30, 1998

Abstract

The beam position measurement system and correction have been investigated in the temporary beam line and high energy experimental area of the TESLA Test Facility Linac. In this report we analyse and present the results obtained on the response of Beam Position Monitors (BPMs), i.e. their range, linearity, resolution and gain. Measurements of the beam response matrix have been carried out and compared with a model of the magnetic layout. An attempt to determine the alignment of BPMs with respect to the magnetic center of quadrupoles was made. The stability of the beam trajectory was studied and its dependence on energy changes in the accelerating module was measured.

1 Introduction

Beam position measurement and correction are issues of increasing importance in the performance of the TESLA Test Facility (TTF) Linac [1] and will play a relevant role in the VUV FEL experiment [2]. In order to apply correction procedures that involve several BPMs and one or several corrector magnets, precise measurements of the beam position and a good knowledge of the matrix transport are required.

The linearity region and the range of beam position measurements is presented in Section 2. The BPM offsets with respect to the magnetic center of quadrupoles can be determined using beam based alignment techniques. The results of such measurement done at one quadrupole doublet located donwstream the accelerating module 1 are presented in Section 3. A schematic view of the TTF Linac (phase I) is shown in Fig. 1.

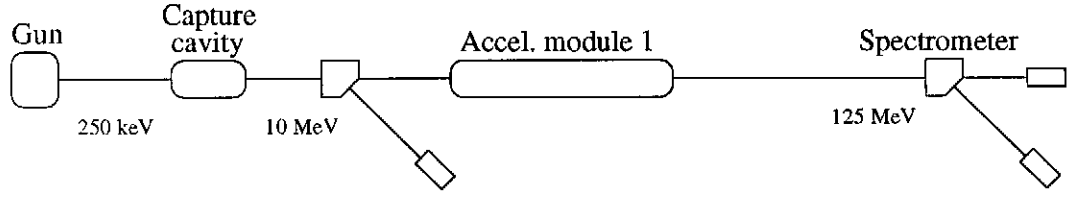

Figure 1: Schematic view of the TTF Linac (phase I).

Beam orbit correction algorithms use the knowledge of the magnetic layout in the form of response matrices (defined in Section 4) in order to find a combination of corrector strengths which reduce the rms beam position offset at the BPMs. Measurements of the response matrices

are compared to model response matrices calculated from quadrupole gradients and measured beam energy. Results on BPM gains, corrector magnet strengths and quadrupole gradients fitted to the measurements are presented in Section 4.

The measurement of the beam trajectory and its correction are affected by position jitter. Instabilities of the beam position affect also the measurement of the beam spot for emittance measurements in both transversal and longitudinal plane. The study of correlated beam position jitter observed at the BPMs is reported in Section 5.

It is foreseen for the beam alignment in the undulator of the FEL to measure and correct the dispersion [3, 4]. A beam energy change of 10% to 20% is required by these procedures. The beam position change due to the change in the accelerating gradient of 10% and 20% has been measured and presented in Section 6.

To introduce the analysis of beam position measurements, we present in the following the layout of the temporary beam line and the high energy analysis area.

1.1 Layout and description of the magnets

The beam position measurements presented in this paper were done at the TTF Linac (phase I) between the last superconducting cavity of module ACC1 and the spectrometer dipole magnet. This area contains the temporary beam line (which will be replaced by the installation of the bunch compressor BC2 and further accelerating modules ACC2 and ACC3) and the high energy analysis area EXP1. The location of magnets and BPMs of the temporary beam line and section EXP1 are shown in Fig. 2 and the description of the components is given in the following section.

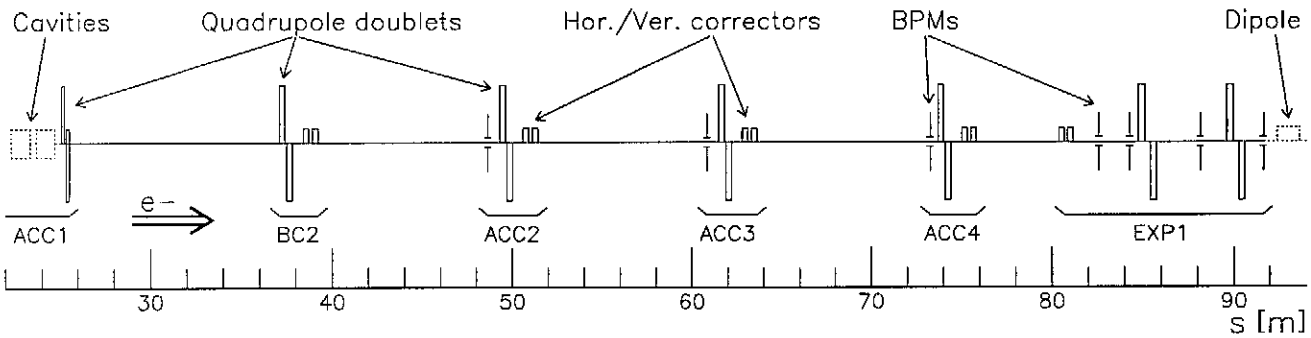

Figure 2: Location of BPMs, quadrupole doublets and corrector magnets in the high energy area of the TTF Linac between the superconducting cavities of module ACC1 and the spectrometer.

1.1.1 Temporary quadrupole doublets

Four pairs of quadrupoles with opposite polarity (doublets) from the firm Danfysik [5] are placed in the temporary beam line. Both quadrupoles in each doublet are connected in series to a single power supply providing a maximum current of 120 A. The distance between the center of the quadrupoles in a doublet is 400 mm. Their effective magnetic length is 304 mm and aperture radius is 30.5 mm. Measurements of the quadrupole gradient g were done for currents I between 0 to 120 A. A fit to these data yields:

$$g = a \cdot I + b \qquad \text{with } a = 0.091 \text{ Tm}^{-1}\text{A}^{-1} \text{ , } b = 0.11 \text{ Tm}^{-1}$$

1.1.2 Protvino quadrupole doublets

Two quadrupole doublets made at Protvino Laboratory are installed at the high energy analysis area EXP1. The maximum current of these doublets is 270 A. The distance between the center of the quadrupoles in a doublet is 650 mm. Their effective magnetic length is 338 mm and the aperture radius is 35 mm. The integrated gradient measured at 235 A is 6.0 T.

1.1.3 Superconducting corrector magnets

Being part of the cryogenic module ACC1, a pair of horizontal and vertical corrector magnets is superimposed to the second quadrupole of the cold doublet. They have the same 150 mm length as the quadrupoles. The maximum current of the wire is 100 A. The integrated field measured at 100 A is $9.59 \cdot 10^{-3}$ Tm.

1.1.4 HERA CV type corrector magnets

Pairs of horizontal and vertical corrector magnets are located at sections BC2, ACC2, ACC3, ACC4 and EXP1 (see Fig. 2). Their effective magnetic length is 300 mm and the distance between the center of the horizontal and vertical magnets is 500 mm. The maximum current is 3.5 A and the integrated field measured at 3 A is $3.0 \cdot 10^{-2}$ Tm.

2 Beam position measurements versus corrector current

There are three stripline BPMs [7, 8] installed in the temporary beam line and four more in the high energy analysis area EXP1. They are 350 mm long and their locations are shown in Fig. 2.

The stripline BPM electronics [9] is designed to cover a range of about ± 1 cm. The BPM response was tested scanning a stretched wire powered with a sinusoidal rf signal. The results presented in [9] show a linear response for wire displacements within ± 5 mm. For displacements larger than 5 mm the BPM response deviates from linear and saturates at a value corresponding to about 10 mm.

This behaviour has been observed at beam position measurements versus steering of corrector magnets. As an example, the beam position measured with the BPM of section ACC2 and averaged over 60 macro-pulses is plotted in Fig. 3 versus the current applied to the horizontal and vertical corrector magnets of section BC2. In the horizontal plane the BPM ACC2 has a linear response in the range of ± 5 mm and in the vertical plane between $+3$ and -5 mm.

3 Quadrupole magnetic center measurement

A beam passing at a distance x_Q from the center of a quadrupole with strength k receives a deflection α

$$\alpha = k \cdot L \cdot x_Q$$

where L is the length of the quadrupole. A change of the quadrupole strength Δk leads to a change of the deflection

$$\Delta\alpha = \Delta k \cdot L \cdot x_Q$$

which is proportional to the beam offset at the quadrupole. The beam deflection at the quadrupole changes the beam trajectory (x and x') at the downstream BPMs. Observing the

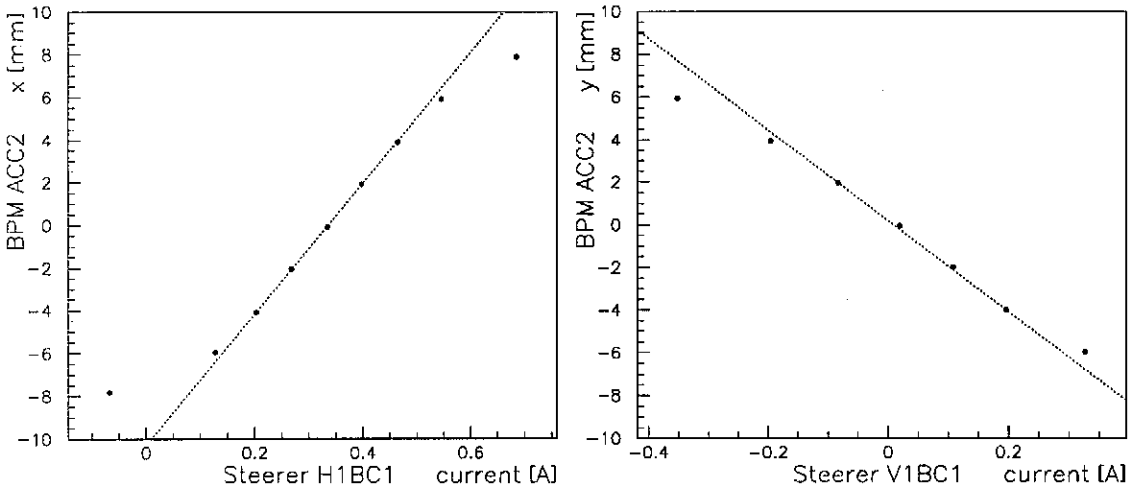

Figure 3: BPM reading versus current of horizontal (left) and vertical (right) correctors.

position shift as a function of the measured position at a BPM close to the quadrupole, one obtains a measurement of the position of the quadrupole magnetic center with respect to the BPM electromagnetic center.

A measurement of the magnetic center of the quadrupole doublet ACC2 with respect to the nearby BPM (see Fig. 2) is reported here. The horizontal and vertical corrector magnets of section BC2 were used to steer the beam position at approximately the 0, ± 2, ± 4 and ± 6 mm readings of the BPM of section ACC2. At each corrector setting, the current of the doublet ACC2 was set at 6.0, 8.0 and 10.0 A and the beam position measured at BPMs located downstream.

As one example of the results obtained, the measured beam position at BPMs ACC2, ACC3 and ACC4 are plotted in Fig. 4 versus the current applied to the vertical corrector magnet of section BC2. A full line is fitted to the black dots, which represent the measured beam position for a doublet current of 8.0 A. A dashed line and a dotted line are fitted to the white dots which represent measurements for a doublet current of 6.0 A and 10.0 A, respectively. The dots which correspond to positions outside the range of linear response of the BPMs (between -5 and 5 mm) are not included into the fits.

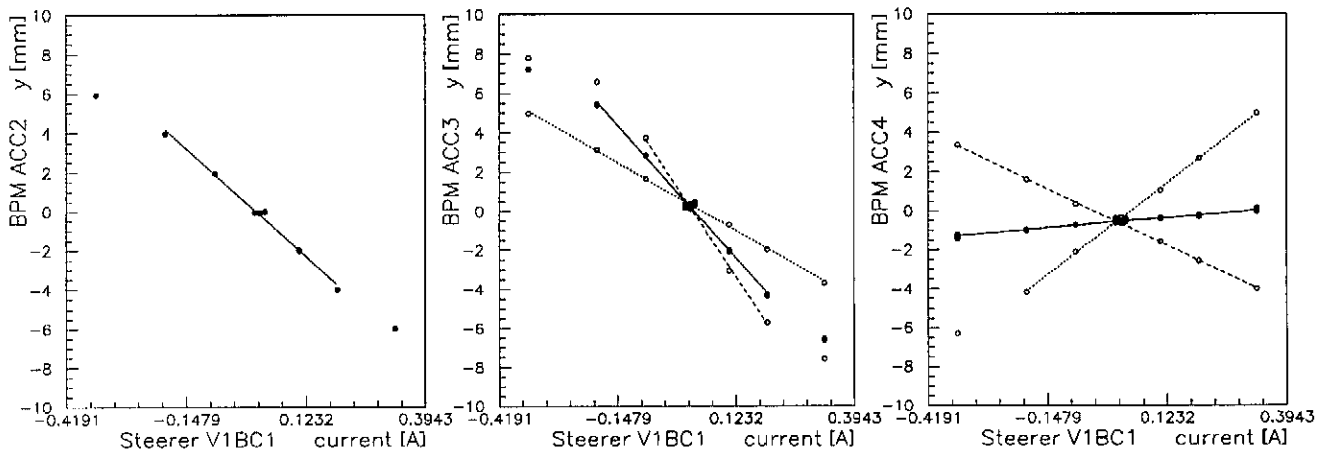

Figure 4: Measured beam position at BPM ACC2 (left), BPM ACC3 (middle) and BPM ACC4 (right) versus current of the vertical corrector of section BC2. The current of the doublet ACC2 was set to 8.0 A (black dots) and to 6.0 A and 10.0 A (white dots).

We also observe the effect of hysteresis on corrector magnets in the three plots shown in Fig. 4. At the center of each plot, where the measured beam position at BPM ACC2 is almost zero, there are similar beam position measurements for different currents of the corrector magnet. The reason is that the beam position was steered initially to 0 mm and increased to 6 mm, steered back to 0 mm and decreased to -6 mm and finally steered again to 0 mm. At each time, the beam position crossed the center of the BPM with a different current on the corrector magnet due to hysteresis.

In order to find the position of the quadrupole magnetic center, the position measurements of BPM ACC4 are plotted in Fig. 5 versus the beam position measured with BPM ACC2. Discarding the position measurements which deviate from a linear behaviour, the best fit of the dashed line ($I = 6.0$ A) and the dotted line ($I = 10.0$ A) coincide at $y \simeq 0.13$ mm. At this point, the position shift due to Δk is expected to be minimum, i.e. the beam is centered at the quadrupole.

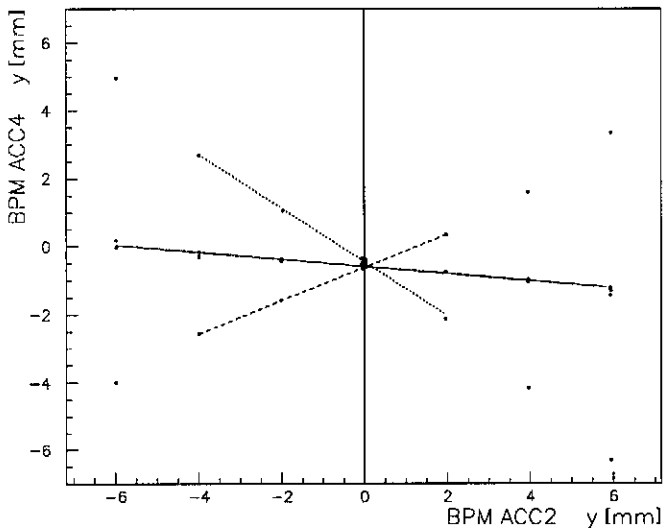

Figure 5: Measured beam position at BPM ACC4 versus measured beam position at the quadrupole doublet ACC2 set to 8 A (full line), 6 A (dashed line) and 10 A (dotted line).

The plot of position measurements of BPM ACC4 vs. BPM ACC2 has been selected for two reasons. First, the position shift due to beam deflections caused by the vertical corrector magnet is small, therefore the beam remains within the linear range of the BPM. Second, the position shift due to quadrupole strength changes is larger than at the other BPMs, which increases the signal-to-noise ratio and, therefore, the resolution of the result. The plot of position measurements of BPM ACC3 vs. BPM ACC2 yields a similar result $y \simeq 0.14$ mm. Looking at the BPMs 3EXP1 and 4EXP1 with a much lower signal-to-noise ratio, we obtain $y \sim 0.09$ mm and $y \sim 0.22$ mm, respectively.

Systematic errors on the determination of the quadrupole magnetic center are mainly due to the angle of the beam trajectory at the BPM ACC2. The longitudinal distance between the center of the BPM and the center of the doublet is about one meter. For an angle of 0.1 mrad, the transverse beam position at the quadrupoles is on average 0.1 mm different from its position at the BPM.

4 Response matrix measurements

4.1 Definition of response matrix

The trajectory of the beam at a longitudinal position s is characterized by its position x and angle x' with respect to the design trajectory. The beam trajectory at positions s_1 and s_2 are related by the transformation matrix (in linear approximation with uncoupled x and y planes)

$$\begin{pmatrix} x_2 \\ x_2' \end{pmatrix} = \begin{pmatrix} R_{11} & R_{12} \\ R_{21} & R_{22} \end{pmatrix} \begin{pmatrix} x_1 \\ x_1' \end{pmatrix} \quad .$$

This matrix is calculated as the product of transformation matrices of each element of the beam line (drift space, quadrupoles) between s_1 and s_2. The expressions for these matrices are given in textbooks (ex. [6]).

The shift of the beam position due to a corrector field located at s_1 is given by the second element R_{12} of the transformation matrix between s_1 and the observation point. The so-called "response matrix", which is used for correcting the beam trajectory, contains the elements R_{12} of the transformation matrices between corrector magnets and BPMs.

4.2 Measurements

Several response matrix measurements were done at the TTF Linac using the corrector magnets in sections ACC1, BC2, ACC2, ACC3, ACC4 and EXP1. The beam displacement introduced by each of these corrector magnets was measured with the BPMs ACC2, ACC3, ACC4 of the temporary beam line and the four BPMs installed in section EXP1. Measured beam positions are averaged over 20 pulses and the rms values (listed in Table 1) are included in eq. 1 as σ_m.

The beam energy is measured from the current reading of the spectrometer. A fit to the measured dipole field versus its current [10] yields

$$E = aI + b \qquad \text{with } a = 7.86 \text{ MeV/A}, b = 0.36 \text{ MeV}$$

Full beam current transmission through the dipole magnet was established and the beam was centered at the BPM located in the dispersion area. The current at the spectrometer was 14.40 A which corresponds to an energy of 113.5 MeV. The error at estimating the beam energy is typically of 2 or 3 percent due to uncertainties in the incident position and angle of the beam trajectory at the entrance of the dipole magnet.

Various current amplitudes (ΔI = 5, 10, 20, 30 and 40 mA) were applied to the corrector magnets to study non-linearities of BPM measurements. The beam position at the BPMs was initially corrected within ± 2 mm.

Comparing the data obtained at the various corrector current amplitudes, we observe that for corrector current changes equal or larger than 20 mA the measured beam shift at some BPMs deviates from linear scaling. At 113.5 MeV, a change of $\Delta I = 20$ mA in a corrector magnet causes a trajectory deflection of 0.52 mrad and a maximum beam displacement of about 5 mm, which is the limit of the linear range of BPMs. In the following we present the analysis of two response matrix measurements that were taken for $\Delta I = 10$ mA and one taken for $\Delta I = 5$ mA.

4.3 Data analysis

In order to obtain detailed information about BPMs, corrector magnets and quadrupole gradients, we compare the measured response matrix with the model response matrix obtained from

transformation matrices.

The beam position shift Δx_{mn} measured with BPM m due to a change in the corrector magnet deflection θ_n is given by

$$\Delta x_{mn} = g_m \theta_n R_{12,mn}$$

where g_m is the gain of BPM m, θ_n is beam trajectory deflection at corrector magnet n and $R_{12,mn}$ is the model response matrix. These parameters g_m and θ_n are varied to minimize the χ^2 deviation between the model and measured response matrices

$$\chi^2 = \sum_{n,m} \frac{(R_{12,mn}(k_i) \cdot \theta_n \cdot g_m - \Delta x_{mn})^2}{\sigma_m^2} \tag{1}$$

where σ_m is the measured beam position error of BPM m. The fit parameters in the model response matrix R_{12} are the strength k_i of both quadrupoles in the doublets BC2, ACC2, ACC3, ACC4, 1EXP1 and 2EXP1. A set of k_i values determines both horizontal and vertical response matrices. Therefore, the measured data in both planes are included in the calculation of χ^2.

The fit parameters g_m and θ_n are inversely correlated. An increase of factor two on the BPM gains can be compensated by including a factor one half on the corrector strengths. Therefore, depending on the initial values given to the fit parameters, a different set of results is obtained. We scale the BPM gains so that the mean value of the gains of BPM ACC2, ACC3, ACC4, 1EXP1 and 2EXP1 is equal to one. Thus, the fit results are unique for a given measurement and the results from analysis of three response matrix measurements are in very good agreement. After scaling also the corrector strengths, the mean value of the θ_n obtained is only a few percent higher than the expected value: it is a 4% higher than the expected value in measurements done with $\Delta I = 10$ mA and 2.6% in the measurement done with $\Delta I = 5$ mA. This result is compatible with an energy error of 2-3%. It also indicates that the calibration of BPMs is on average very good. However, the rms value of θ_n is about 7%, which is larger than the magnetic field errors expected ($< 1\%$). A reason for that can be hysteresis effects on corrector magnets.

Results of BPM gains are shown in Table 1. The rms value of gains of the "reference" BPMs ACC2, ACC3, ACC4, 1EXP1 and 2EXP1 is about 6%. The results for gains of BPMs 3EXP1 and 4EXP1 are not included in the calculation of the mean value.

		horiz. gain				vert. gain		
BPM	σ_x [mm]	I	II	III	σ_y [mm]	I	II	III
ACC2	0.030	1.08	1.09	1.08	0.025	0.92	0.92	0.91
ACC3	0.060	0.89	0.89	0.89	0.035	0.98	0.98	0.98
ACC4	0.070	0.98	0.98	0.96	0.020	1.03	1.04	1.01
1EXP1	0.020	1.05	1.04	1.05	0.025	1.06	1.06	1.07
2EXP1	0.025	1.00	1.00	1.02	0.027	1.01	1.01	1.03
3EXP1	0.035	1.88	1.95	1.84	0.033	1.84	1.83	1.87
4EXP1	0.025	1.21	1.15	1.15	0.025	1.08	1.09	1.07

Table 1: Results for BPM horizontal and vertical gains from analysis of three response matrix measurements: applying $\Delta I = 10$ mA (columns I and II) and applying $\Delta I = 5$ mA (column III) on corrector magnets.

The BPM gains resulting from the fit are found to be correlated to the range of their beam position readings, i.e. the distance between their minima and maxima. The maximum and

minimum reading values obtained from BPMs during various runs over several days are listed in Table 2. The largest range (about ±15 mm) is found at the horizontal measurements of BPM 1EXP3. The gains of the BPMs versus their range is plotted in Fig. 6.

BPM	min. x	max. x	min. y	max. y
ACC2	-8.1	9.0	-7.0	6.0
ACC3	-7.4	7.6	-8.2	7.8
ACC4	-7.2	7.6	-8.7	6.3
1EXP1	-8.8	9.3	-8.7	8.3
1EXP2	-7.3	7.8	-8.5	7.5
1EXP3	-14.4	16.7	-13.7	11.6
1EXP4	-11.8	9.1	-5.6	10.0

Table 2: Maximum and minimum readings of BPMs. The actual maxima and minima of BPMs can be, however, larger than the values presented in this table.

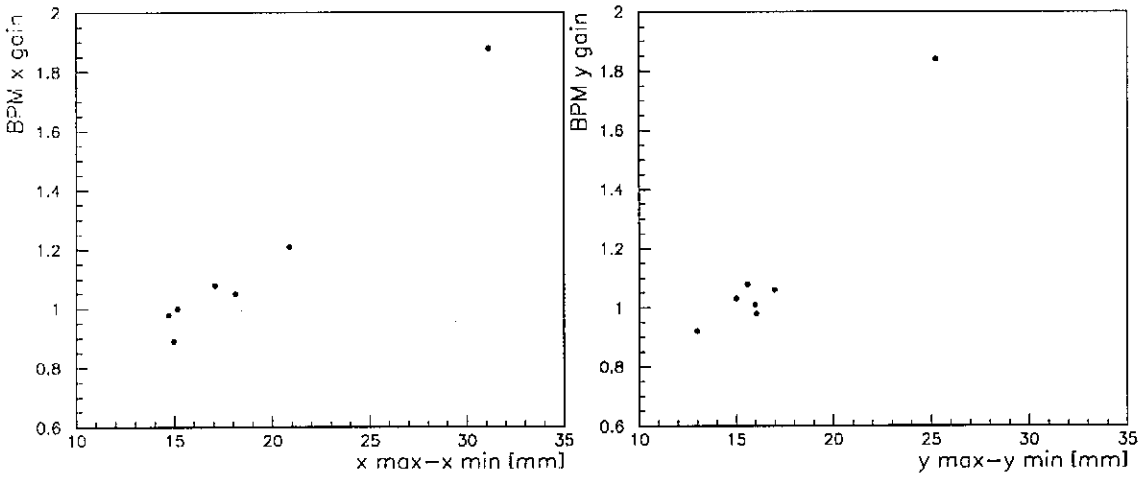

Figure 6: BPM gain versus BPM range for horizontal (left) and vertical (right) planes.

Results of the fit for doublet gradients k_i are shown in Table 3.

The expected gradients for the temporary quadrupoles are about 0.12 Tm^{-1} higher than the results of the three fits. However, the expected gradients of Protvino quadrupoles are only about 2% higher than fitted ones, which can be attributed to measurements errors or an energy uncertainty. The error on temporary quadrupoles appears to be systematic and independent of the quadrupole current.

The results of the fit and the expected gradients of both quadrupole types versus their currents are shown in Fig. 7. While the expected gradient of temporary quadrupoles has an offset value at zero current, the results of the fit are lying on a calibration line which is consistent with having vanishing gradient for zero current. As previously mentioned in section 1.1, magnetic bench measurements of temporary quadrupole were carried out applying currents from 0 to 120 A and ramping down to 0. After this cycle, a remanent field of 0.11 Tm^{-1} is observed probably due to hysteresis. The typical range of currents used in phase I of the TTF Linac are from 0 up to 10 or 20 A, not large enough to excite the remanent field observed in the bench tests.

As an example of the results obtained, the measured position change due to corrector magnet H1BC2 and the expected trajectory displacement of the fitted model are shown in Fig. 8.

Quad.	I[A]	g[T/m]	meas. g I	II	III	Δg
BC2	8.001	0.838	0.736	0.744	0.738	0.099
ACC2	8.024	0.840	0.705	0.703	0.705	0.136
ACC3	7.996	0.838	0.727	0.732	0.724	0.110
ACC4	8.991	0.928	0.808	0.807	0.807	0.121
1EXP1	13.463	1.023	1.002	1.002	1.002	0.021
2EXP1	18.231	1.386	1.379	1.362	1.364	0.018

Table 3: Expected quadrupole gradients g (calculated from their current I) and gradients fitted to measurements with $\Delta I = 10$ mA (columns I and II) and $\Delta I = 5$ mA (column III).

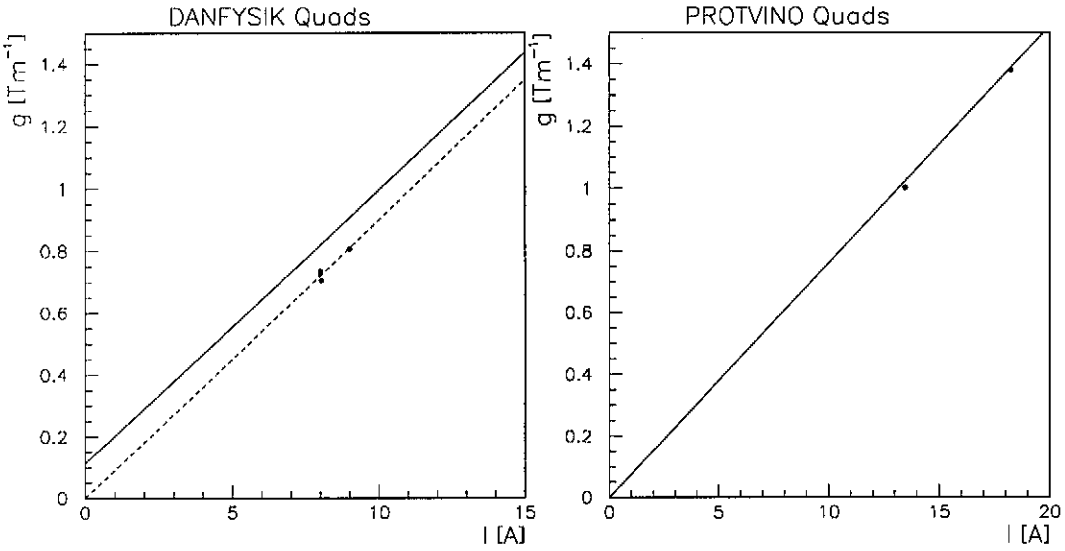

Figure 7: Gradient versus current for temporary (left) and Protvino (right) quadrupoles. The dashed line on the left plot is $g = aI$ with a=0.09 $\mathrm{Tm^{-1}A^{-1}}$. The dots are the fitted gradient of each quadrupole.

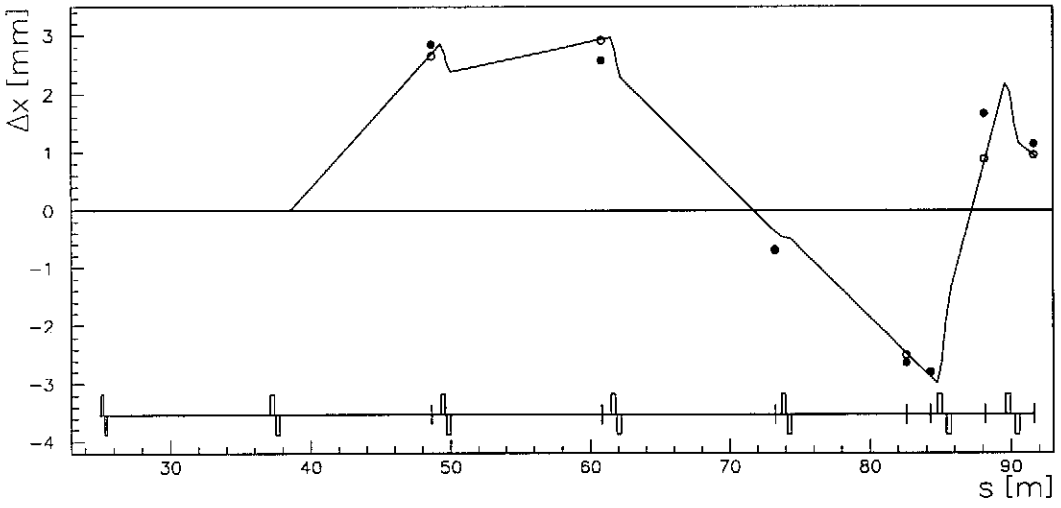

Figure 8: Horizontal trajectory displacement due to a current change on the corrector magnet at section BC2. Measured position changes are marked with black dots. White dots indicate same measurements including gain correction. (The beam line layout is given in Fig. 2.)

5 Beam position jitter

The stability of BPM measurements was studied during periods of synchrotron light experiments at the spectrometer, when linac manipulations were seldom applied. Correlated beam position jitter was observed in most of the BPMs and at both horizontal and vertical planes. Moreover, the position jitter is partially correlated with variations of the beam current (which was measured after module 1).

The position jitter observed at the BPMs corresponds to variations of the beam trajectory. In order to analyse this jitter and determine its origin, a trajectory is fitted to the beam position at the BPMs obtained at each measurement minus the average position over 100 measurements. The values of the BPM gains used in the fit are from Table 1 and the gradients of temporary quadrupoles is calculated from Fig. 7. As an example, the measured jitter $\Delta x_m = x_m - < x_m >$ (with m being the BPM index) and the fitted trajectory are shown in Fig. 9. The error bars associated to the measured position jitter represent the size of the LSB (least significant bit), which is 0.024 mm for BPMs ACC2, ACC3, ACC4, 1EXP1 and 2EXP1 and is 0.041 mm for BPMs 3EXP1 and 4EXP1.

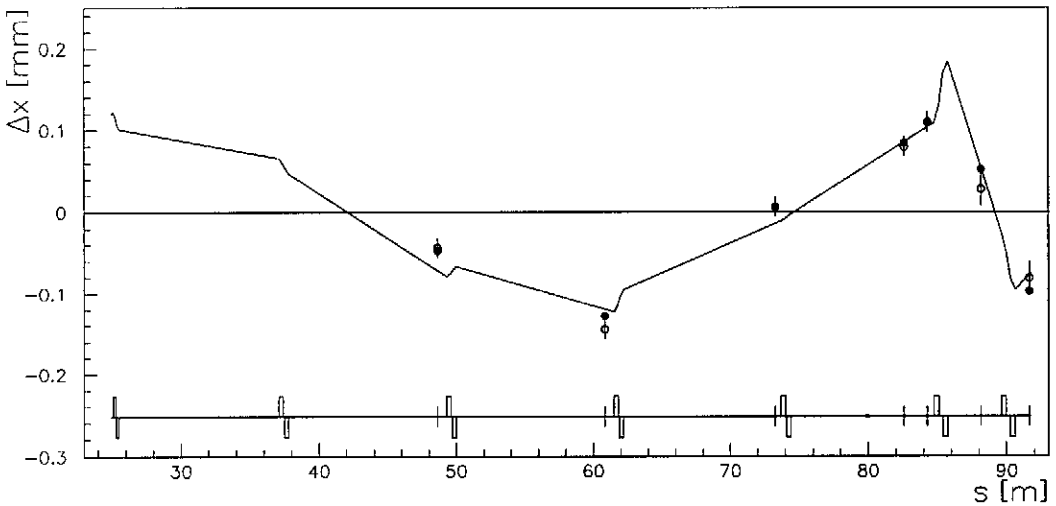

Figure 9: Beam trajectory fitted to $\Delta x_m = x_m - < x_m >$, where x_m is the horizontal beam position measured with BPM m. Black dots represent Δx_m and white dots are $\Delta x_m / g_m$ (g_m being the gain of BPM m given in Table 1).

Some of the largest amplitudes of jitter were observed at position measurements taken on 17th July. The rms values of the measured position are up to 0.2 mm in the vertical plane. The fitted trajectories of 100 position measurements are shown in Fig. 10.

The fitted beam trajectory to each measurement can be represented as a betatron oscillation around the average trajectory with a certain amplitude and phase. We observe in Fig. 10 that all beam jitter trajectories have about same phase and random amplitude. At approximately $s = 42$, 75 and 89 m the beam position jitter is almost zero (nodes), that is, the oscillation has a phase of $\phi = 0$ or 180°. If the origin of the beam jitter is unique, the source introduces a random kick on the beam trajectory which is located upstream with a phase advance of $n \times 180°$ from these nodes. Moreover, the stripline BPM 1INJ3 located at the entrance of module 1 presents a position jitter which is correlated to the measurements with BPMs in the beam line. Therefore, the origin of beam jitter has to be located in the injection section.

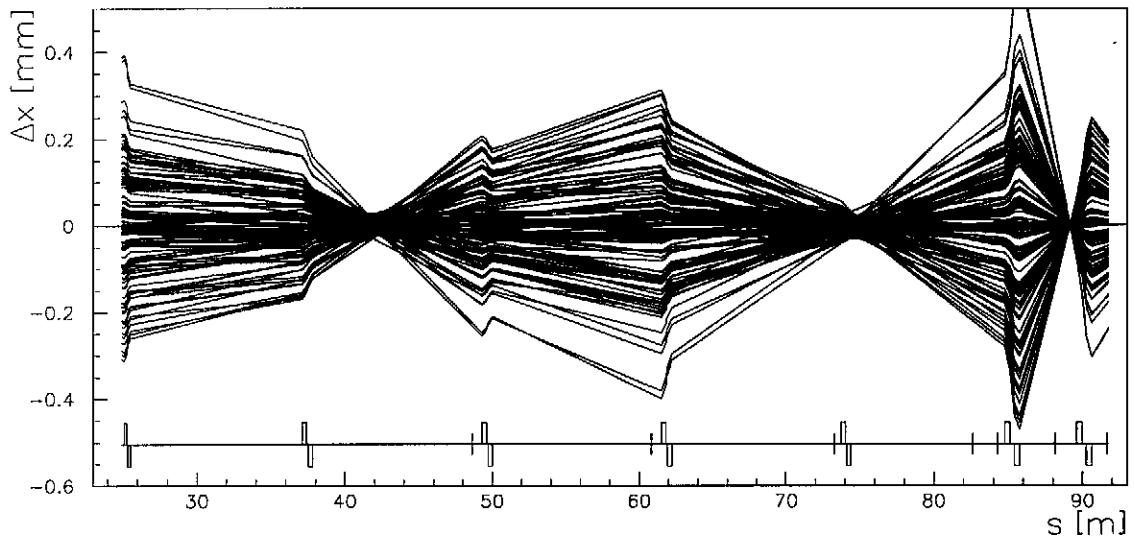

Figure 10: Beam trajectory jitter. Each line corresponds to the fitted trajectory to position jitter of BPM measurements.

6 Beam dispersion

A change of the accelerating gradient or phase in the module 1 introduce some distortions on the beam trajectory due to misalignments of the cavities in the module. Additionally, the beam deflection of corrector fields and beam position offsets in quadrupoles is inversely proportional to the beam energy, which is known as beam dispersion. For small energy changes (a few percent) the position change is linear with the relative energy change. If the energy decreases more than a few percent, the focusing strength of quadrupoles is stronger and the beam trajectory oscillates more rapidly.

The change of the beam position was measured at the BPMs for a change on the accelerating gradient of 10% and 20% are shown in Fig. 11. We observe that the position change in the first monitor (ACC2) is almost linear, while in the rest of the monitors the position change is highly non-linear due to the change of the phase advance.

7 Conclusions

Stripline BPMs are used in the temporary beam line and in the high energy experimental area of TTF linac. Their linearity, range, gain and stability has been studied in this report. The stripline BPMs provide a linear response in the range of about ±5 mm. The saturation of the BPM signal corresponds to a reading of about ±10 mm. A relative gain has been determined from measurements of the response matrices. Except for BPM 3EXP1, the relative gain error is within ±10%. The gain error of BPM 3EXP1 is almost a factor two larger, which explains the larger range of its reading values. A mapping of the response of the BPMs using corrector magnets is therefore a very useful tool to determine their linear region and find large gain errors.

A measurement of the magnetic center of quadrupole ACC2 with respect to the nearby BPM resulted on about 0.13 mm. However, a beam trajectory angle of 0.1 mrad introduces a systematic error of 0.1 mm in this measurement, since the BPM and the center of the quadrupole doublet are about 1 m apart.

Quadrupole gradient and corrector strengths are fitted in order to compare model and mea-

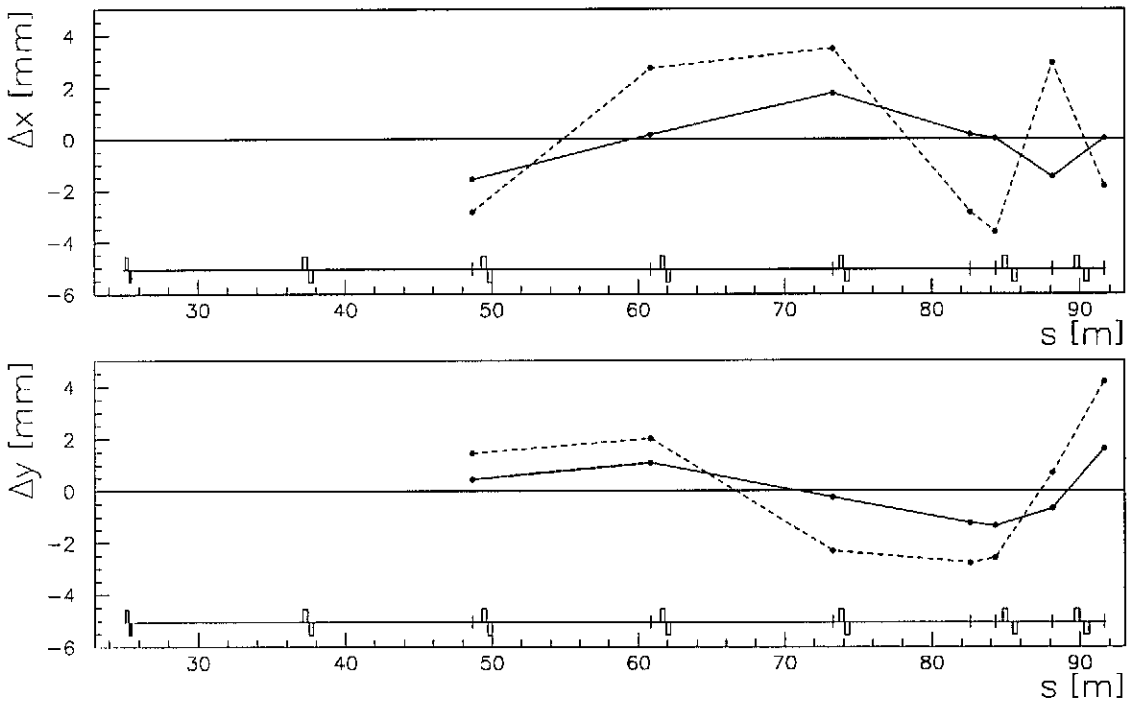

Figure 11: Measured change of the beam position in the horizontal (upper plot) and vertical (lower plot) due to a change on the accelerating gradient of 10% (full line) and 20% (dashed line).

sured response matrices. Results for temporary quadrupole gradients are lower than expected. The expected gradients result from magnetic measurements using currents between 0 and 120 A, while the range of currents used are between 0 and 10 A. The gradient difference, as well as the large rms value of fitted corrector strengths (about 7%), are probably due to hysteresis effects. In principle, it is possible to extend this technique to model the transport matrix through module 1 from the values of cavity acceleration fields and phases.

Based on the pattern of correlated jitter observed at the BPMs we conclude that the jitter has its origin on a single point in the injector section. To determine the source of jitter will require a model of the transport matrix through module 1 and the use of BPMs in the injector section.

A measurement of the beam position change due to a change of 10% and 20% on the accelerating gradient of module 1 is presented. For a 10% change in gradient, a position shift up to 2 mm was measured in both planes.

References

[1] *TESLA Test Facility Linac, Design Report*; DESY/TESLA-FEL 95-01, March 1995.

[2] *A VUV Free Electron Laser at the TESLA Test Facility at DESY, Conceptual Design Report*; DESY/TESLA-FEL 95-03, June 1995.

[3] P. Castro, *TTF FEL Beam Based Alignment by Dispersion Correction using Micado algorithm*, DESY TESLA-FEL 97-04, August 1997.

[4] K. Flöttmann, B. Faatz, E. Czuchry and J. Roßbach, *Beam Based Alignment Procedure for an Undulator with Superimposed FODO Lattice*, DESY TESLA-FEL 97-05, December 1997.

[5] Danfysik A/S, Mollehaven 31, Jyllinge, Denmark.

[6] H. Wiedemann; *Particle Accelerator Physics*; Ed. Springer-Verlag. 1993.

[7] R. Lorenz, M. Sachwitz, H. J. Schreiber and F. Tonisch; *Measurement of the beam Position in the TESLA Test Facility Linac*; Proc. of the LINAC 96, Geneva, pp. 527-529.

[8] M. Castellano et al.; *First Operating Experiences of Beam Position Monitors in the TESLA Test Facility Linac*; Proc. of the PAC 97, Vancouver.

[9] M. Castellano, L. Catani, M. Ferrario, P. Patteri and F. Tazzioli; *Tesla Test Facility Stripline Readout System*; Proc. of the EPAC 96, Barcelona, pp. 1633-1635.

[10] TTF Linac log-book; entry on 4th June 1997.